

## NEAR Optical Navigation at Eros

W. M. Owen, Jr., T. C. Wang  
Jet Propulsion Laboratory, California Institute of Technology  
4800 Oak Grove Dr.  
Pasadena, CA 91109-8099

A. Harch, M. Bell, C. Peterson  
Cornell University  
Ithaca, NY

Successful navigation of the spacecraft NEAR Shoemaker during its orbit phase at the asteroid Eros depended critically on optical navigation. The irregular shape of Eros and its large apparent size precluded the use of traditional optical navigation techniques whereby the center of mass of a target body is located relative to stars in onboard imaging. Rather, optical navigation during NEAR's orbit phase consisted of locating small craters in images of Eros' surface and using those landmarks to infer Eros' rotation state, the body-fixed coordinates of each landmark, and the trajectory of the spacecraft.

### Introduction

The NEAR navigation team relied heavily on optical navigation (“opnav”) data during the terminal approach to Eros and the subsequent yearlong orbital operations.<sup>1</sup> Opnav provided direct observations of NEAR Shoemaker's position relative to certain craters or “landmarks” on the surface of Eros, enabling rapid orbit determination (OD) updates after maneuvers and generally providing important constraints on the OD solutions throughout the orbit phase. Since the inertial position of surface features depends on Eros' rotational state, opnav data were also useful to provide initial estimates of Eros' pole orientation.

This paper describes the challenges of obtaining useful navigation data from close-range pictures of an asteroid. We describe the software advances and the operational procedures that were developed to do the job, and we present the results of our efforts.

### Opnav challenges at Eros

Traditional opnav processing<sup>2</sup> relies on imaging a target body against a background of reference stars whose coordinates are well known. The star images provide a direct measurement of the inertial orientation of the onboard camera (the “Multispectral Imager” or MSI<sup>3</sup>), and the target body images provide information on both the spacecraft's position and the target's position. This technique was used for Mariner 9, Viking 1 and 2, Voyager 1 and 2, and Galileo. We used it for NEAR's flyby of Mathilde<sup>4</sup> and for the approach to Eros, while the asteroid's image was small compared to the camera's field of view.

We note in passing that “the target's position” above refers to the position of the center of mass of the target. For nearly spherical large bodies, the center of mass is usually close enough to the center of figure that the latter is a useful quantity to measure, and it is straightforward to infer the location of the center of figure in an image. Mathilde never subtended more than a couple of pixels in the pre-encounter opnavs, but the relatively slow relative velocity on approach to Eros meant that we'd resolve the asteroid for several months before encounter. The first challenge at Eros, then, was to find a way of inferring the center of Eros from images that showed only the irregularly shaped lit limb and even more irregular terminator.

Another challenge arose from the high surface brightness of Eros. The short exposures that were necessary to avoid overexposing Eros were not long enough to capture any but the very brightest stars, and the probability of finding a useful star image was vanishingly small. Alternate methods of determining the camera's inertial attitude had to be found.

Beginning in the last few days before orbit insertion, and throughout the yearlong orbital phase that followed, NEAR Shoemaker could image only a small part of the surface. Opnav during the orbit phase thus had to consist of locating craters or "landmarks" in the images; the software would in effect deduce the position of the spacecraft relative to the center of Eros by using the landmarks as intermediaries. This technique of course requires that both the body-fixed coordinates of the landmarks and the rotation state of Eros be adequately known. Although the machinery for processing landmark observations had been included in the opnav software for 15 years, the NEAR mission marked the first operational use of landmarks.

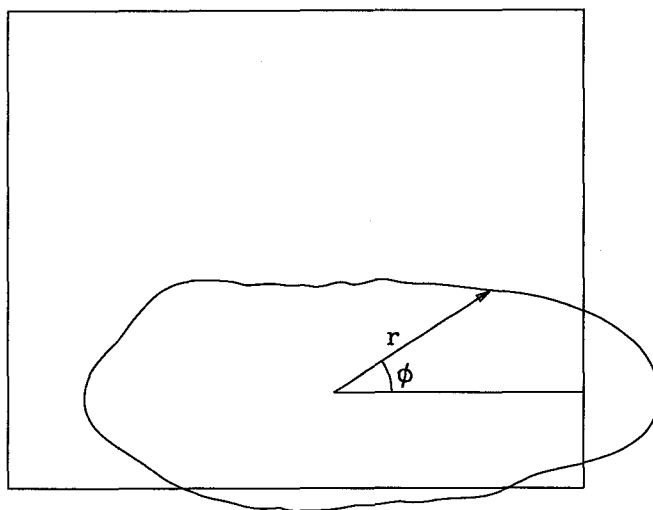
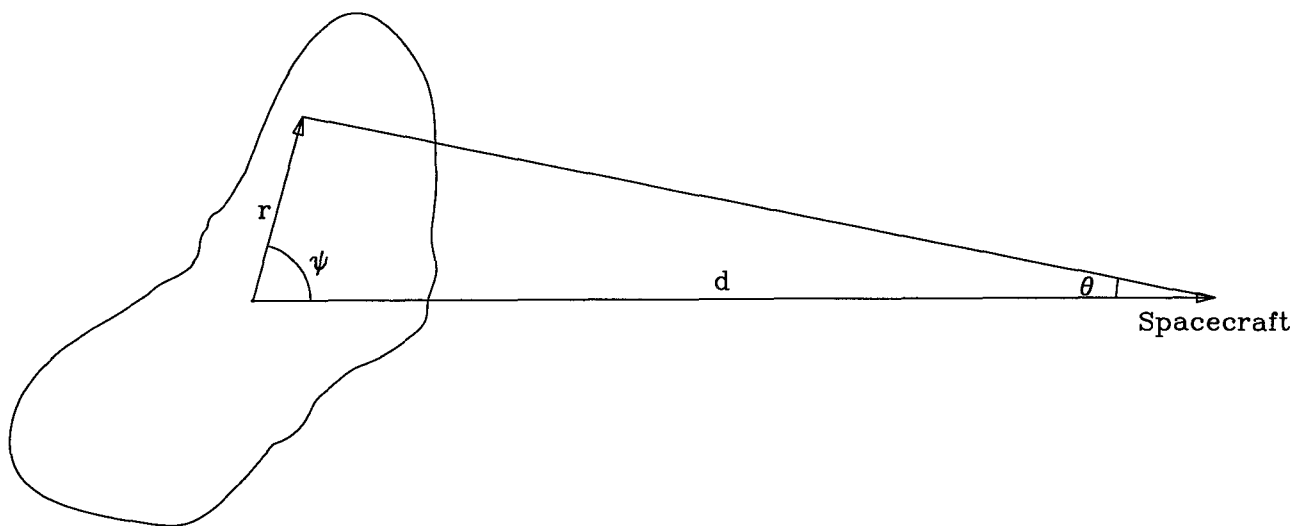
Finally there was the issue of the image processing itself: how to determine an accurate measurement of the  $(x, y)$  coordinates of a crater image. These measurements, however made, must show no systematic effects depending on the particular geometry of any one picture; there must be no significant dependence on either shadowing (angle of incidence) or foreshortening (angle of emission). An even more fundamental question was the identification problem: each observation of a given landmark must always refer to the same feature out of the tens of thousands of craters on Eros.

### NEAR-specific software development

Most of the challenges discussed above were met through either modifications to an existing image display program or development of a landmark database and associated software. The software work was largely completed by December 1998, when NEAR was originally to have been placed into orbit around Eros. The aborted maneuver and subsequent recovery and redesign of the mission<sup>5,6</sup> gave us one more year to continue upgrading the software.

The image display program was originally written in a mixture of Fortran and assembly language in the 1970s to run on a Modcomp IV minicomputer and peripherals. It was rewritten completely in Fortran in the 1980s for VAX machines and rewritten again for Sun and HP workstations in the early 1990s. The current version is mostly in C, with calls to X and Motif functions, although some of the low-level geometry routines are still in Fortran. The original purpose of the code, maintained through the decades, was to allow an analyst to display an image with the predicted locations of stars or Solar System objects overlaid on it, move those overlays to match the picture, and save the results for use by subsequent centerfinding programs. Three major capabilities were added for NEAR.

First, we incorporated a shape model, based on spherical harmonics, for Eros. The shape model itself was produced by Thomas<sup>7</sup>, and other members of the navigation team at JPL determined its spherical harmonic coefficients. This shape model was used to predict the profile of Eros' limb as follows (see Fig. 1): Let  $\mathbf{d}$  be the vector from the center of mass of Eros to the spacecraft camera. Define a plane containing  $\mathbf{d}$  such that the projection of that plane into the camera focal plane makes an arbitrary angle  $\phi$  with the  $x$ -axis of the picture. Define a vector  $\mathbf{r}$ , lying in this plane, making an angle  $\psi$  with the direction from the camera to Eros, with origin at Eros' center of mass. The length  $r$  of this vector is found from the shape model, and the angle  $\theta$  between  $\mathbf{d}$  and  $(\mathbf{d} - \mathbf{r})$  is the apparent separation between the center of Eros and the surface for that  $\mathbf{r}$ . Vary  $\psi$  between 0 and 180°, and the maximum value of  $\theta$  determines the location of the limb for the chosen value of  $\phi$ . Vary  $\phi$  between 0 and 360° and one obtains the desired set of limb points. These are then



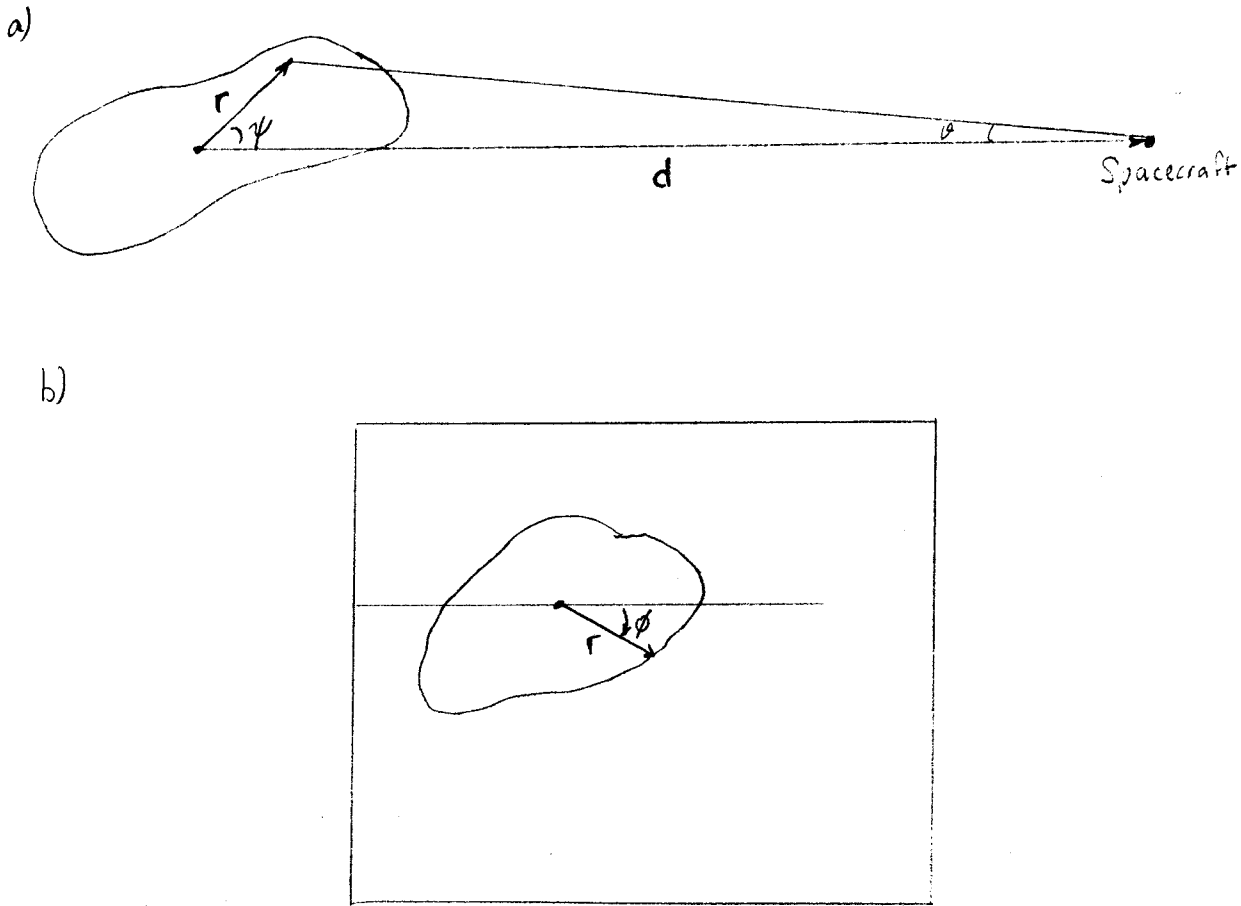
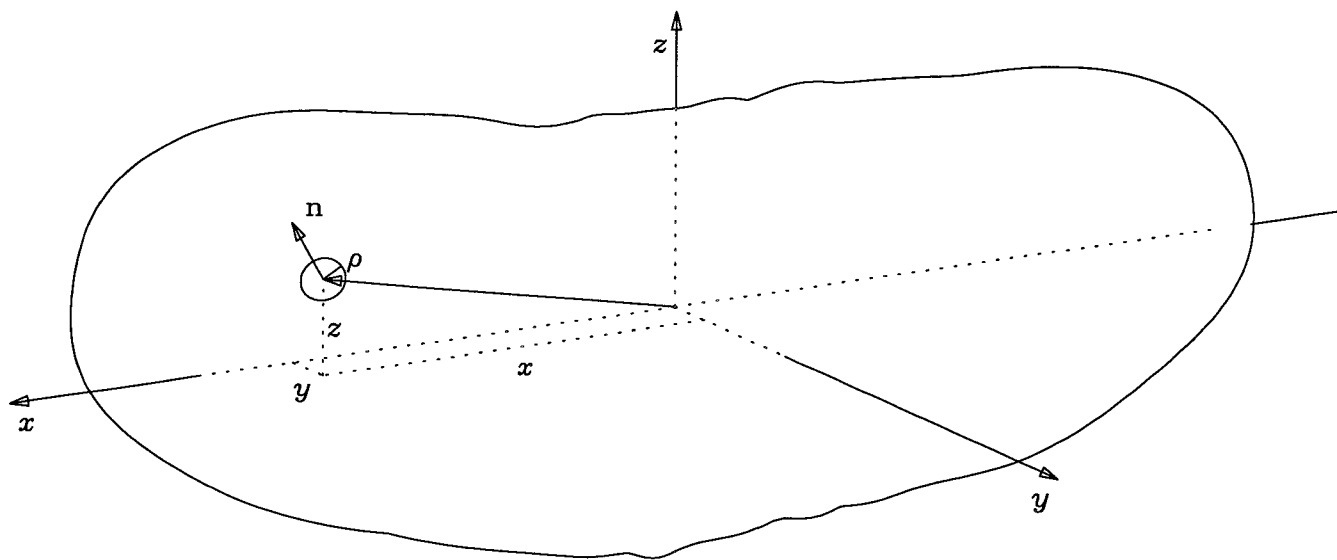


Figure 1. The geometry for determining the location of a point on the limb of an irregularly-shaped body, *a*) as seen in three dimensions and *b*) as projected into the image.

mapped into  $(x, y)$  coordinates in the camera focal plane in the usual manner and are plotted as the overlay for Eros.

Second, we added the capability of displaying overlays for the landmarks at their correct size and orientation. Landmarks are modeled as circles in three dimensions. The landmark is described by a vector from the center of mass of Eros to the center of the circle, the radius  $\rho$  of the circle, and the latitude  $\varphi$  and longitude  $\lambda$  of the vector  $\hat{n}$  normal to the plane containing the circle (Fig. 2). All these are given in body-fixed coordinates. The position and orientation of the landmark in inertial space therefore also depend on the orientation of Eros itself. Since the landmark is modeled as a circle, its projection into the focal plane of the camera is an ellipse. The image display software calculates the size, shape, and orientation of that projected ellipse and displays it as the overlay. The radius and orientation of the landmark were used only for display purposes; only the coordinates of the point at the center of the circle were used in navigation.

The third and most important enhancement to the image display software was the addition of computer-aided crater centerfinding. We chose this approach rather than a completely automated centerfinding technique because the latter could not have been developed in time for this mission. The computer-aided approach required a significant amount of work by two opnav analysts during the final approach and orbital phases of the mission, but it worked well and produced good results.



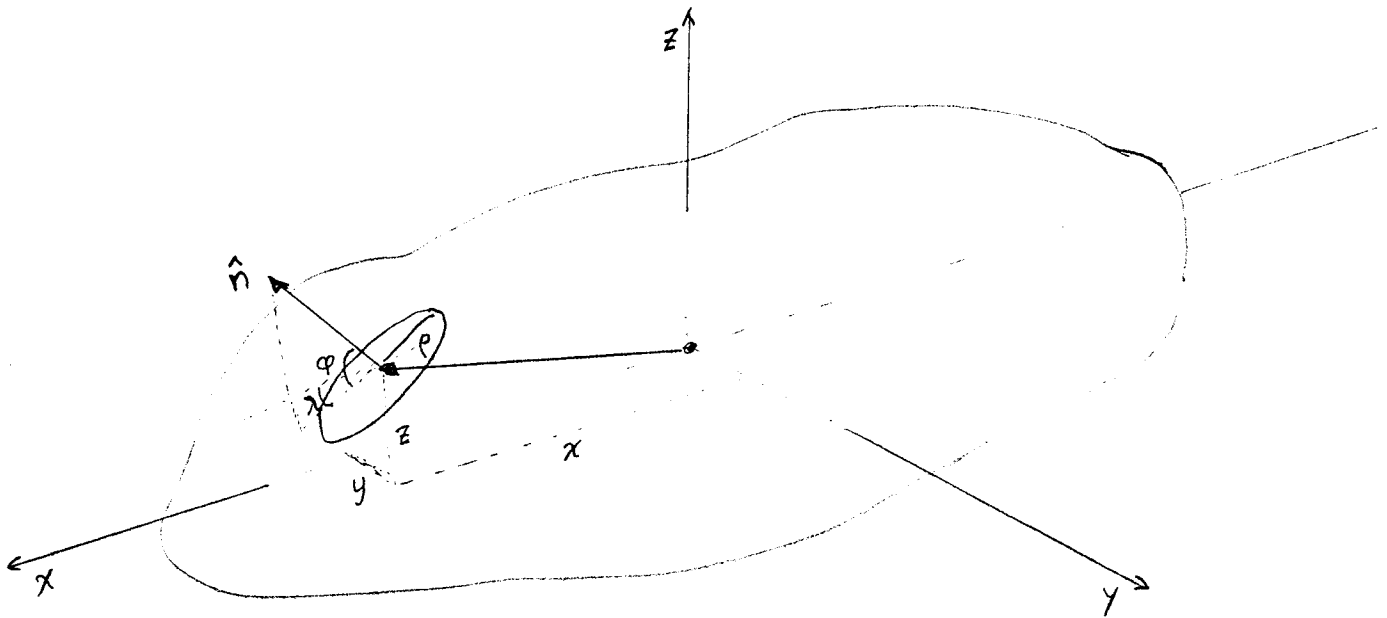


Figure 2. A landmark is modeled as a circle on the surface of Eros.

The analyst would measure a crater by dragging the cursor around the rim of the crater. The software would record each point over which the cursor moved and fit an ellipse to that set of points. The center of the best-fit ellipse is taken to be the observed center of the landmark. (Because the rim of a crater lies above the floor of the crater, the fiducial point corresponding to the center of the landmark generally lies some distance above the actual surface of Eros.) The shape and orientation of the projected ellipse give the size of the crater and two solutions for its orientation in space. The more plausible orientation, in which the side closer to the camera is also closer to the apparent center of Eros, is chosen by default, but the user can override that choice. The software also determines the body-fixed coordinates of the landmark center by determining the place where the ray emanating from the camera, in the direction defined by the coordinates of the landmark image, intersects the shape model. After the user has approved the results, the program writes one record to an output observation file; this record contains the picture ID and the landmark's name, its  $(x, y)$  coordinates, its body-fixed vector, its radius, the body-fixed orientation of its normal vector, and the body-fixed vector from the landmark to the camera.

To keep track of the thousands of landmarks expected to be identified on Eros required a rudimentary database capability. One master file contained for each landmark a name, the model parameters (body-fixed coordinates, radius, and normal vector) as described above, and a count of the number of times it was observed. This text file was then used to produce a set of consistent files giving the same information in formats peculiar to the various programs that needed it. Approximately twenty small utility programs were written to handle the various aspects of file formatting, data transfer, database update, and the like.

### Planning opnav pictures

Because the camera footprint was so small, planning opnav images required special care. The camera budget allowed three sets of opnav pictures daily, each set containing two mosaics aimed at widely separated landmarks. It was challenging to find landmarks whose angles of incidence and emission were favorable. Planning was therefore also computer-aided. Many science images were also used for navigation purposes.

*Most of this section to be written by Ann Harch. She will describe the procedures and software that the Cornell folks used, the varying schemes for taking opnav frames throughout the approach and orbit phases, and the process of incorporating the opnav requests into the sequences. She, Maureen Bell, and Colin Peterson did the picture planning under JPL's direction.*

## Image centerfinding

All image processing used picture files that had been calibrated by removal of dark current, image readout smear, and pixel nonuniformities.<sup>8</sup> The calibration process was performed on computers belonging to NEAR's Science Data Center, located at the Applied Physics Laboratory, and the resulting image files were then transferred over the Internet to JPL for analysis. We did not attempt to rectify the pictures, as there were concerns that the geometric fidelity of star images might be compromised. Rather, the analysis software accounted for the rectangular shape of the pixels ( $27 \times 16 \mu\text{m}$  in the focal plane), and we learned to live with distorted displays in which each pixel appeared as a square.

Three techniques were used to locate the centers of images in NEAR pictures. Star centers were found by fitting a two-dimensional Gaussian plus constant background to the observed DN values in a  $15 \times 15$  array of pixels centered on the approximate location of the star image. The modeled intensity at any point was

$$I(x, y) = I_s \exp \left[ -\frac{1}{2} \left( \frac{x - x_s}{\sigma_x} \right)^2 - \frac{1}{2} \left( \frac{y - y_s}{\sigma_y} \right)^2 \right] + b,$$

where  $I_s$  and  $b$  are the central intensity of the star and the background level,  $(x_s, y_s)$  are the coordinates of the star image, and  $\sigma_x$  and  $\sigma_y$  are the standard deviations of the star profile in the  $x$  and  $y$  directions. The predicted value for the DN in each pixel is the integral of  $I(x, y)$  over the photosensitive part of that pixel. We held  $\sigma_x$  and  $\sigma_y$  constant at 1.7 and 1.0 pixels, respectively, and obtained  $x_s$ ,  $y_s$ ,  $I_s$ , and  $b$  from a least-squares solution. The solution was iterated until convergence was achieved. The resulting centroids  $(x_s, y_s)$  exhibited postfit residuals typically 0.1 to 0.2 pixel in each coordinate, because most of the stars were observed at a S/N ratio of less than 3. Centroiding for brighter stars was much more accurate, at about 0.05 pixel. The degraded point-spread function of the camera hurt the star centroiding, but that turned out not to be the limiting error source.

Image coordinates for the center of mass of Eros were found by eye. An analyst would move the overlay for Eros' limb, computed as described above, until the overlay matched the observed lit limb in the picture. The terminator was not used. This technique was used during the initial approach to Eros, before craters became visible. The results were repeatable to better than 0.5 pixel, but errors in the pre-encounter shape model introduced systematic errors, depending on rotational phase, in the observed centroids. These errors probably amounted to slightly more than one pixel.

The centroiding process for landmarks was likewise computer-aided, using the enhancements to the image display software described above. An analyst would display each image in turn and drag the cursor around the rim of each crater to be measured. Software would fit an ellipse through these points and display it on the image. If the fit appeared reasonable, the measurement was accepted, and the center of the fitted ellipse was saved as the desired image center. Over 134,000 measurements were made in this way between 2000 February 3 (eleven days before orbit insertion) and the end of the mission on 2001 February 12. The inferred centers of small craters were reproducible to about 0.25 pixel, based on analysis of repeated pictures taken in rapid succession.

The accuracy degraded for larger images. We adopted a data weight  $\sigma$  that depended on the apparent size  $d$  of the landmark:

$$\sigma = [(1.0 \text{ pixel})^2 + (0.1 d)^2]^{1/2}.$$

This data weighting scheme was probably slightly conservative, especially for small well-defined craters.

The limiting error source in the opnav measurements turned out to be our ability to infer the camera attitude from the telemetered spacecraft attitude. By the time of the last pictures before orbit insertion, Eros filled a significant fraction of the field of view, and scattered light from the asteroid washed out the stars. From that point onward we never saw Eros and stars in the same picture, and we were forced to use indirect methods to obtain the camera attitude. The onboard attitude control system used star tracker and gyro data to obtain the attitude of the spacecraft itself, or more precisely, the attitude of the star tracker. The camera and the star tracker were mounted on different parts of the spacecraft, and their relative attitude was not constant; it would change as the aft deck of the spacecraft flexed due to temperature changes. We monitored the camera offset angles daily, by taking pictures of a star field and comparing the actual camera attitude to that predicted from the spacecraft attitude. These corrections were then applied to all the landmark pictures taken on that day. Errors in the daily calibration amounted to about one pixel.

### Landmark data processing

We knew from simulations that craters would first become visible when Eros was about 30 or 40 pixels across, that we would see the northern hemisphere on approach, but that after orbit insertion we'd see Eros from a completely different perspective. The design of the orbital phase called for a gradual reduction in the semimajor axis of the orbit, to allow progressively better determination of the gravity field as well as higher resolution imaging. We planned to use the largest craters initially and to survey the visible surface of Eros each time the orbit shrank. Stereo imaging, necessary to obtain all three components of each landmark vector, would initially be obtained from a set of images taken during one rotation of Eros. Additional imaging as the spacecraft flew over different latitudes in its orbit would then improve the solution. Landmarks identified at one altitude would be useful in the next lower orbit. We planned the last global survey for an altitude of 100 km, expecting that a complete map at 50 km would require too many pictures and take too much time; the 100 km map would have to serve in all lower orbits. We followed this plan with only minor changes.

The first four craters, between 1 and 2.5 km radius in the then-sunlit northern hemisphere, became apparent 11 days before orbit insertion. The spacecraft was then within 9000 km of Eros, the asteroid's apparent diameter was 40 pixels, and the body-centered latitude of the spacecraft was  $+44^\circ$ . We used several movie sequences first to find the landmarks and then to solve jointly for their body-fixed coordinates and for the inertial direction of Eros' rotation pole. In this geometry we could get good solutions for the pole, for the longitude of each crater and for its distance from Eros' spin axis, but the distance of each crater from Eros' equator was not well determined. By the time of orbit insertion we had identified over 50 landmarks, of which the best 27 were used by the navigation team.

There was a 35-hour interval before orbit insertion, including the "low-phase flyover," during which imaging was not possible. After insertion the spacecraft was flying along Eros' terminator, above the south side of the asteroid, and looking partly at new (to us) terrain and partly at known features



from a completely different perspective, and all from about 400 km, closer than ever before. We hurriedly used a rotation movie to find about 200 new landmarks in Eros' equatorial regions.

New landmarks were added to the database when the spacecraft orbital radius was decreased to 200 and 100 km, again using a rotation movie both for identification and for the initial solution for the landmark vectors. In June 2000 the sun crossed Eros' equator, fully illuminating the southern side of the asteroid, and that occasioned one last campaign of crater identification from an orbital altitude of about 100 km.

Landmark vectors were obtained from a least-squares solution in which the only other parameters were the right ascension and declination of Eros' spin axis and the prime meridian angle  $W_0$  at epoch J2000.0. Initially the  $y$  coordinate of a large crater near the prime meridian was held fixed, implicitly defining the zero point of the longitude system. Once the navigation team had a reliable determination of the location of Eros' principal axes, these defined  $x$  and  $y$ , we stopped estimating  $W_0$ , and we allowed all the landmark longitudes to vary.

The final landmark database, shown in Fig. 3, contained 1624 entries, but due to limitations on the turnaround time no more than 44 at a time could be used for orbit determination. It was immediately apparent that the best craters for navigation purposes were small, circular, and relatively deep, with no interference from neighboring craters, yet with enough craters and other features nearby to make identification easy. Only a few of the initial 80 craters were of high quality, but several of the equatorial craters found in the 400 km orbit served for the remainder of the mission. Most of the 1624 landmarks were used only to provide context for the few good ones.

The set of 44 "navigation landmarks" changed during the course of the mission, following the sun from the north to the south side of the asteroid. Larger craters were replaced by smaller ones as these became available. During the last two months of the mission, when the spacecraft was in a retrograde equatorial orbit and the sun was over Eros' south pole, nearly all of the navigation landmarks were just south of the equator. Only three craters first seen at 400 km just after orbit insertion were still usable by the end of the mission.

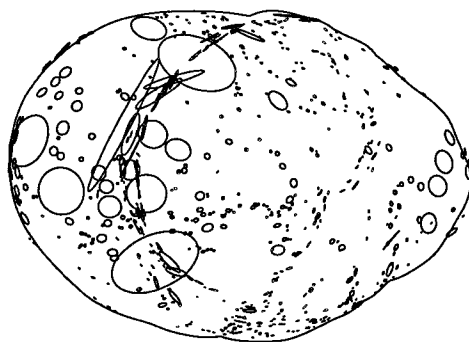
## Conclusions

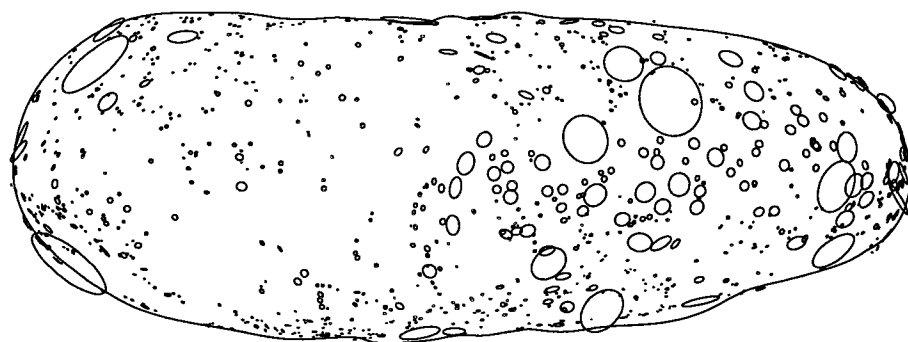
The opnav team at JPL processed nearly 34,000 pictures during the approach and orbital phases of the NEAR mission (Table 1). This total includes not only the star fields used to calibrate the camera pointing and all of the imaging planned specifically for opnav but a good fraction of the science pictures as well. We identified nearly 1600 landmarks on Eros' surface, and we obtained an average of over 80 observations of each one. Six of the best landmarks were observed over 500 times each.

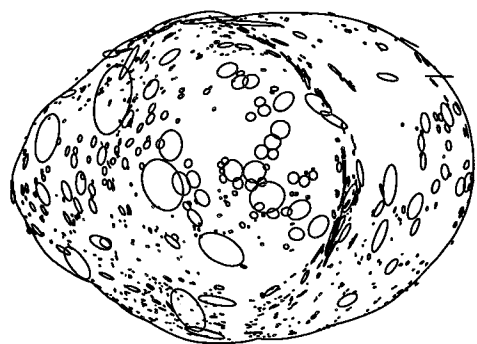
The MSI team at Cornell prepared input for approximately sixty onboard sequences, usually working on four different one-week sequences simultaneously. Their continual attention to detail and their willingness to adapt their procedures as the mission progressed produced a nearly perfect dataset.

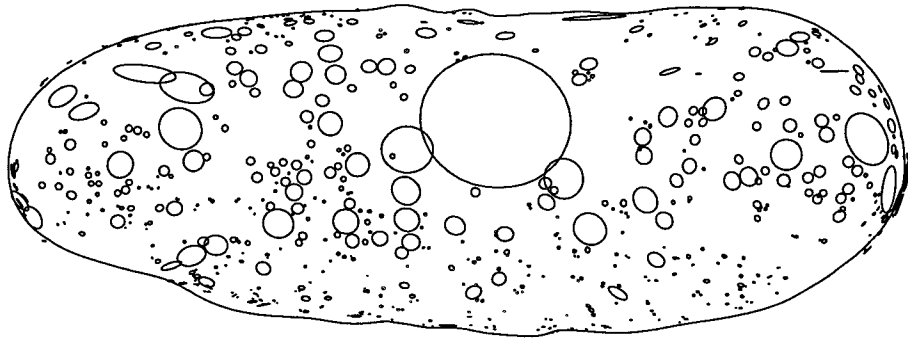
Close cooperation between the JPL and Cornell teams was essential. The two groups were in frequent communication throughout the mission, and they developed an excellent rapport despite the physical distance separating them. Consequently no opnav pictures were lost due to a lack of understanding by the sequencers. NEAR marked the first time JPL delegated the opnav sequencing authority to external providers, and this decision was borne out by the success of the mission.

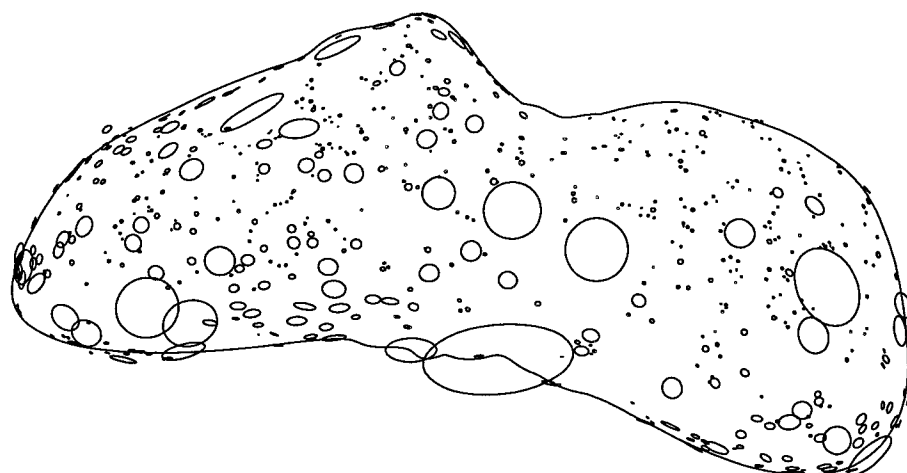
Because of the volume of data analyzed, and the great pains taken to plan and acquire the images, the body-fixed coordinates of the landmarks were obtained to a typical accuracy of 1 meter (one

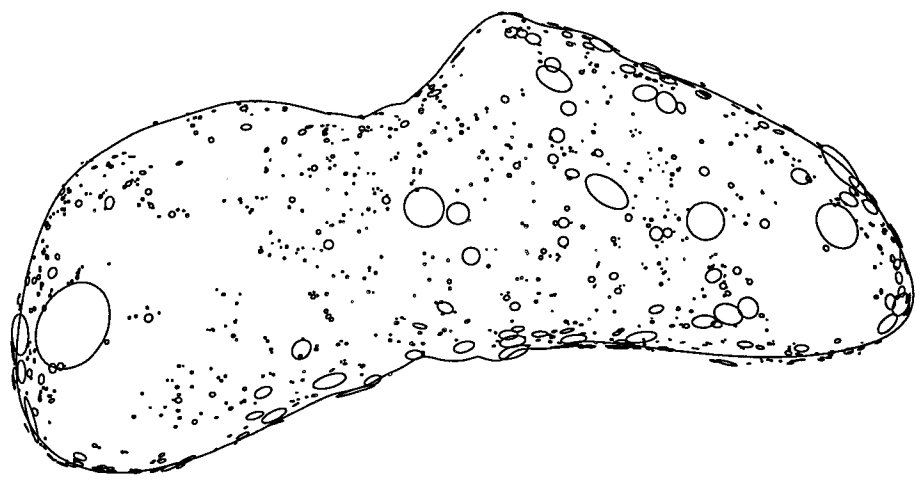












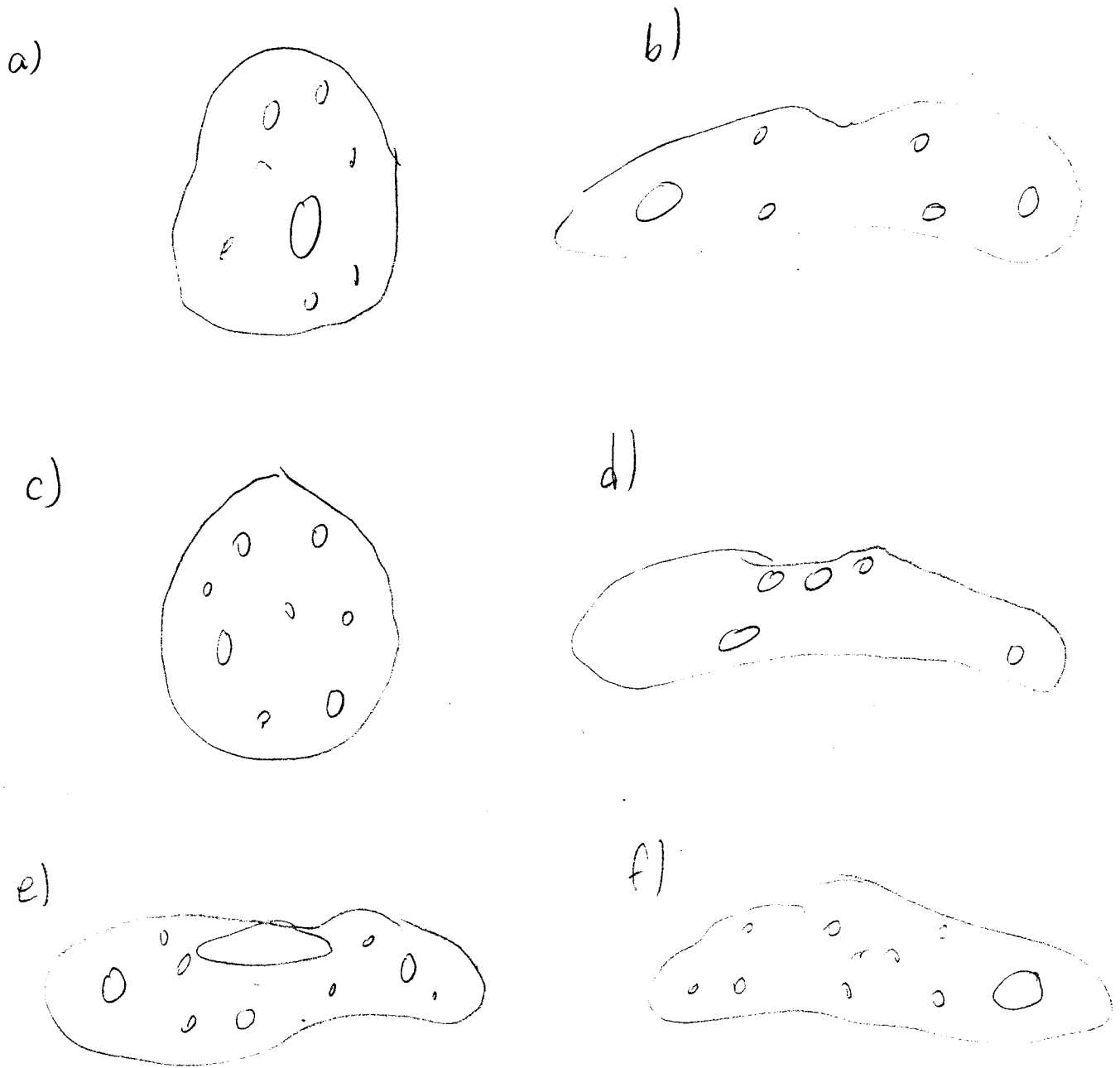


Figure 3. The 1624 landmarks in the final database. These are plotted as seen from *a*) the positive  $x$ -axis, *b*) the positive  $y$ -axis, *c*) the negative  $x$ -axis, *d*) the negative  $y$ -axis, *e*) the positive  $z$ -axis (above Eros' north pole), and *f*) the negative  $z$ -axis.



Table 1. NEAR optical navigation statistics

Total number of pictures taken starting Dec. 17, 1999	181,393
Number of pictures we downloaded to JPL for analysis	33,968 (18.73%)
Number of useful pictures (at least 1 landmark)	17,601
Number of accepted pictures (some had bad attitude)	17,352
Number of on-orbit star calibration sequences	314
Number of star calibration pictures	1,424
Number of valid landmarks in database	1,590
Number of landmark observations	134,267
Number of misidentified landmark observations	1,314 (0.98%)
Number of landmark observations in pictures with bad attitude	1,616 (1.20%)
Number of useful landmark observations	131,337 (97.82%)
Average number of useful observations per landmark	82.6
Average number of useful observations per picture	7.6

sigma). Conversely, the opnav data were used to locate the spacecraft to an uncertainty of about 10 meters (one sigma), a record for spacecraft not orbiting the Earth.

The opnav process for NEAR Shoemaker at Eros—principly the identification and cataloguing of 1600 landmarks, and the processing of over 130,000 observations of them—worked as expected, with few surprises. The results were excellent, enabling the NEAR navigation team to deliver accurate OD solutions at least twice a week for a year. Future missions would do well, however, to automate the onerous task of determining the coordinates of landmarks in the imaging data. This was the most labor-intensive part of the process. Although the human hand and eye could achieve results easily adequate for the navigation of this mission, effort spent in automation would pay off in reduced operations costs and perhaps even more reliable data.

## Acknowledgments

We wish to thank Brian Carcich (Cornell) for invaluable programming support throughout the NEAR mission but especially for his timely upgrades to the picture planning software. Mark Robinson (Northwestern) wrote the IDL scripts used to perform photometric calibration of the MSI images. Eric Carranza (JPL) wrote the program which reformats spacecraft trajectory files for use in the opnav system. Doug Holland and the Science Data Center at APL, with Mark Holdridge and the Mission Operations team, provided the image data.

Part of the research described in this paper was carried out by the Jet Propulsion Laboratory, California Institute of Technology, under a contract with the National Aeronautics and Space Administration.

## References:

1. Williams, B. G. *et al.* 2001. "Navigation for NEAR Shoemaker: the First Mission to Orbit an Asteroid," this conference.
2. Riedel J. E. *et al.* 1990. "Optical Navigation During the Voyager Neptune Encounter," AIAA paper 90-2877, AIAA/AAS Astrodynamics Conference, Portland, Oregon.

3. Hawkins, S. E. *et al.* 1997. "Multi-Spectral Imager on the Near Earth Asteroid Rendezvous Mission," *Space Sci. Rev.* 82, 101.
4. Scheeres, D. J. *et al.* 1998. "Mission Design and Navigation of NEAR's encounter with Asteroid 253 Mathilde," AIAA paper 98-184, AIAA/AAS Space Flight Mechanics Meeting, Monterey, California.
5. Veverka, J. *et al.* 1999. "NEAR's Flyby Reconnaissance of Asteroid 433 Eros: Imaging and Spectral Results," *Science* 285, 562.
6. Dunham, D. W. *et al.* 2000. "Recovery of NEAR's Mission to Eros," *Acta Astronautica* 47, 503, and references therein.
7. Thomas, P. 2000. Personal communication.
8. Murchie, S. *et al.* 2001. "Inflight Calibration of the NEAR Multispectral Imager, 2: Results at Eros," *Icarus*, in press.